

AD-A142 536

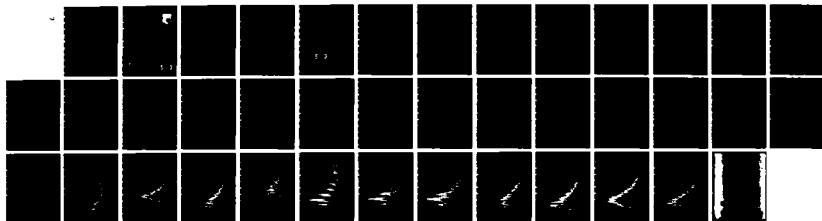
CO2 GAMMA 3 FUNDAMENTAL BAND 45 MICROMETERS LASER
POTENTIAL(U) CALSPAN ADVANCED TECHNOLOGY CENTER BUFFALO
NY J W RICH ET AL MAR 84 CALSPAN-7176-A-1
AFWAL-TR-84-1033 F33615-83-C-1048

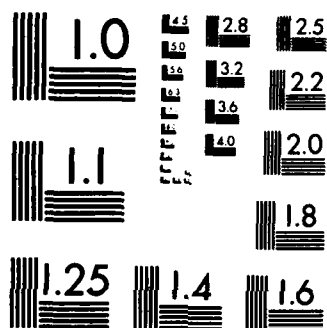
1/1

UNCLASSIFIED

F/G 7/4

NL



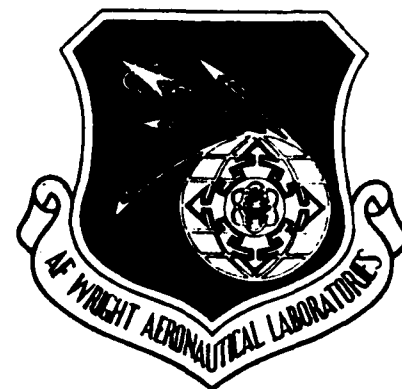


MICROCOPY RESOLUTION TEST CHART
NATIONAL BUREAU OF STANDARDS-1963-A

(12)

AFWAL-TR-84-1033

AD-A142 536



CO₂ ν_3 FUNDAMENTAL BAND 4.5 μ m LASER POTENTIAL

J.W. Rich
R.C. Bergman

Calspan Advanced Technology Center
P.O. Box 400
Buffalo, New York 14225

March 1984

Final Report for Period 5/2/83 to 3/26/84

Approved for public release; distribution unlimited

DTIC FILE COPY

AVIONICS LABORATORY
AIR FORCE WRIGHT AERONAUTICAL LABORATORIES
AIR FORCE SYSTEMS COMMAND
WRIGHT-PATTERSON AIR FORCE BASE, OHIO 45433

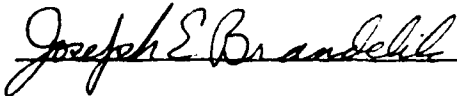
DTIC
ELECTE
JUN 28 1984
B

NOTICE

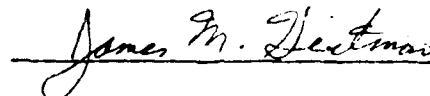
When Government drawings, specifications, or other data are used for any purpose other than in connection with a definitely related Government procurement operation, the United States Government thereby incurs no responsibility nor any obligation whatsoever; and the fact that the government may have formulated, furnished, or in any way supplied the said drawings, specifications, or other data, is not to be regarded by implication or otherwise as in any manner licensing the holder or any other person or corporation, or conveying any rights or permission to manufacture use, or sell any patented invention that may in any way be related thereto.

This report has been reviewed by the Office of Public Affairs (ASD/PA) and is releasable to the National Technical Information Service (NTIS). At NTIS, it will be available to the general public, including foreign nations.

This technical report has been reviewed and is approved for publication.

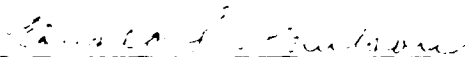


Joseph E. Brandelik
Project Engineer
Electro-Optic Sources Group



James M. Heitman, Chief
Electro-Optic Sources Group
Electro-Optic Technology Branch

FOR THE COMMANDER



Ronald F. Paulson, Chief
Electro-Optic Technology Branch
Electronic Technology Division

"If your address has changed, if you wish to be removed from our mailing list, or if the addressee is no longer employed by your organization please notify AFWAL/AANDC, W-PA/B, OH 45433 to help us maintain a current mailing list".

Copies of this report should not be returned unless return is required by security considerations, contractual obligations, or notice on a specific document.

REPORT DOCUMENTATION PAGE

1a. REPORT SECURITY CLASSIFICATION UNCLASSIFIED			1b. RESTRICTIVE MARKINGS NONE		
2a. SECURITY CLASSIFICATION AUTHORITY			3. DISTRIBUTION/AVAILABILITY OF REPORT Approved for public release; distribution unlimited		
2b. DECLASSIFICATION/DOWNGRADING SCHEDULE					
4. PERFORMING ORGANIZATION REPORT NUMBER(S) 7176-A-1			5. MONITORING ORGANIZATION REPORT NUMBER(S) AFWAL-TR-84-1033		
6a. NAME OF PERFORMING ORGANIZATION Calspan Advanced Technology Center		6b. OFFICE SYMBOL (If applicable)	7a. NAME OF MONITORING ORGANIZATION Avionics Laboratory AFWAL/AADO-1 Air Force Wright Aeronautical Laboratories Air Force Systems Command		
6c. ADDRESS (City, State and ZIP Code) Buffalo, New York 14225			7b. ADDRESS (City, State and ZIP Code) Wright-Patterson Air Force Base Ohio 45433		
8a. NAME OF FUNDING/SPONSORING ORGANIZATION		8b. OFFICE SYMBOL (If applicable)	9. PROCUREMENT INSTRUMENT IDENTIFICATION NUMBER F 33615-83-C-1048		
8c. ADDRESS (City, State and ZIP Code)			10. SOURCE OF FUNDING NOS.		
			PROGRAM ELEMENT NO.	PROJECT NO.	TASK NO.
			61101F	ILIR	83
11. TITLE (Include Security Classification) CO ₂ v ₃ Fundamental Band 4.5 μm Laser Potential			WORK UNIT NO. 04		
12. PERSONAL AUTHOR(S) Rich, J.W., Bergman, R.C.					
13a. TYPE OF REPORT Final		13b. TIME COVERED FROM 2 May 83 TO 31 May 84		14. DATE OF REPORT (Yr., Mo., Day) 2 Apr 84 MARCH 1984	
				15. PAGE COUNT 38	
16. SUPPLEMENTARY NOTATION					
17. COSATI CODES			18. SUBJECT TERMS (Continue on reverse if necessary and identify by block number)		
FIELD	GROUP	SUB. GR.	INFRARED LASER		
2005			INFRARED SPECTROSCOPY		
			CO ₂ Laser		
			Vibrational Energy Transfer		
19. ABSTRACT (Continue on reverse if necessary and identify by block number)					
<p>→ This report presents results of an experimental program to explore the lasing potential of the CO₂ (0,0,V₃) → CO₂ (0,0,V₃-1) asymmetric stretch bands in a cooled electrical glow discharge. The CO₂ (0,0,V₃) level populations were measured by infrared emission spectroscopy from V₃ = 1 to V₃ = 10. The influence of flow velocity, discharge current density, and wall temperature on the populations was measured. It was found that these states do enter a vibration-to-vibration pumped partial population inversion, which is enhanced at lower temperatures. However, states above V₃ ≈ 10 do not appear pumped, and the inversion was insufficient to achieve laser oscillation in the apparatus used. Alternate experimental configurations which may achieve lasing on these bands are suggested.</p>					
20. DISTRIBUTION/AVAILABILITY OF ABSTRACT UNCLASSIFIED/UNLIMITED <input checked="" type="checkbox"/> SAME AS RPT. <input type="checkbox"/> DTIC USERS <input type="checkbox"/>			21. ABSTRACT SECURITY CLASSIFICATION UNCLASSIFIED		
22a. NAME OF RESPONSIBLE INDIVIDUAL BRANDELIK, J.E.			22b. TELEPHONE NUMBER (Include Area Code) 513-255-3804		22c. OFFICE SYMBOL AFWAL/AADO-1

TABLE OF CONTENTS

<u>SECTION</u>		<u>PAGE</u>
I	INTRODUCTION AND BACKGROUND	1
II	CO ₂ ² ₃ MODE POPULATION DISTRIBUTIONS AND CALCULATED SMALL SIGNAL GAIN	3
III	EXPERIMENTS	7
	1 LARGE BORE TUBE	7
	2 COMPARISON WITH COMPUTED SYNTHETIC SPECTRA	9
	3 SMALL BORE TUBE	11
	4 GAIN ESTIMATES AND LASER OSCILLATION EXPERIMENTS	12
IV	SUMMARY AND CONCLUSIONS	14
	REFERENCES	16

DTIC
ELECTE
JUN 28 1984
S **D**
B



Accession For	
DTIC	<input checked="" type="checkbox"/>
DTIC TAB	<input type="checkbox"/>
Unannounced	<input type="checkbox"/>
Justification	
PER CALL JC	
By	
Distribution/	
Availability Codes	
Avail and/or	
Dist	Special
A-1	

LIST OF TABLES

<u>Table No.</u>	<u>Title</u>	<u>Page</u>
1	CO ₂ ν_3 Band Wavelengths	6
2	Operating Parameters, 2 cm Dia. Tube Measurements	8
3	Emission Intensity Ratios, Theoretical Comparison	9
4	Operating Parameters, 1 cm Dia. Tube Measurements	11

LIST OF ILLUSTRATIONS

<u>Figure No.</u>	<u>Title</u>	<u>Page</u>
1	CO ₂ (0,0,V ₃) Populations Measured by Dang et al.	17
2	Calculated Small Signal Gain on (0,0,V ₃) → (0,0,V ₃ -1) Transitions for Data of Dang et al.	18
3	Theoretical Predictions of (0,0,V ₃) Population Distributions	19
4	Calculated Small Signal Gain on (0,0,V ₃) → (0,0,V ₃ -1) at 250°K	20
5	Calculated Small Signal Gain on (0,0,V ₃) → (0,0,V ₃ -1) at 150°K	21
6	IR Emission Spectrum, 2 cm Tube, Slow Flow	22
7	IR Emission Spectrum, 2 cm Tube, Room Temperature	23
8	IR Emission Spectrum, 2 cm Tube, Dry Ice Cooling	24
9	IR Emission Spectrum, 2 cm Tube, Liquid Nitrogen Cooling	25
10	Synthetic CO ₂ (ν ₃) IR Spectrum for 150°K	26
11	Synthetic CO ₂ (ν ₃) IR Spectrum for 250°K	27
12	Synthetic CO ₂ (ν ₃) IR Spectrum for 350°K	28
13	IR Emission Spectrum, 1 cm Tube, Dry Ice Cooling	29
14	IR Emission Spectrum, 1 cm Tube, Liquid Nitrogen Cooling	30
15	IR Emission Spectrum, 1 cm Tube, Dry Ice Cooling, Purged Optics	31
16	IR Emission Spectrum, 1 cm Tube, Dry Ice Cooling, Purged Optics, Low Current Density	32

Section I

INTRODUCTION AND BACKGROUND

Since 1976, a number of new lasing transitions have been reported on infrared bands of the CO_2 molecule, in addition to the $10.4\text{ }\mu\text{m}$ $(001) \rightarrow (100)$ and $9.4\text{ }\mu\text{m}$ $(001) \rightarrow (02^{\circ}0)$ transitions. These include the $(100) \rightarrow (01^1_0)$ cascade band at $14\text{ }\mu\text{m}$,¹⁻³ the $(101) \rightarrow (011)$ difference band at $17\text{ }\mu\text{m}$,⁴ the $(00n) \rightarrow (1,0,n-1)$ and $(00n) \rightarrow (0,2,n-1)$ sequence bands in the $9\text{--}11\text{ }\mu\text{m}$ region,⁵⁻⁷ and the $(10^{\circ}1, 02^{\circ}1) \rightarrow (10^{\circ}0, 02^{\circ}0)$ cascade bands at $4.3\text{ }\mu\text{m}$.⁸⁻¹⁰

It was pointed out by Reid and Siemsen⁶ that the inversion on the $(00n) \rightarrow (0,2, n-1)$ sequence bands is created in an electric glow discharge for conditions in which the $\text{CO}_2 \nu_3$ mode temperature (as measured between $00^{\circ}2$ and $00^{\circ}1$) is $\sim 4000^{\circ}\text{K}$, while the gas translational temperature is kept at $\sim 250^{\circ}\text{K}$ by wall-cooling the discharge with a dry-ice methanol mixture. Such conditions favor vibration-vibration (V-V) collisional pumping of the higher anharmonic vibrational states $(00n)$ of the ν_3 mode. This V-V pumping mechanism¹¹ is responsible for the population inversions among the anharmonic vibrational states of carbon monoxide in the $5\text{ }\mu\text{m}$ CO infrared laser.¹² Accordingly, it was suggested in Ref. 6 that a partial inversion among the higher $(00n)$ states of the $\text{CO}_2 \nu_3$ mode, sufficient to create lasing on the $(0,0,n \rightarrow 0,0,n-1)$ $\text{CO}_2 \nu_3$ band, might exist in such a cooled electric discharge.

Quite recently, Dang, Reid, and Garside¹³ measured the detailed vibrational population distribution of the $\text{CO}_2 \nu_3$ mode $(00n)$ states from $n = 0$ to $n = 9$ in a cooled glow discharge, and demonstrated that the distribution is indeed V-V pumped in accordance with the theoretical model of Ref. 11. These results are reviewed below.

Initial attempts to obtain lasing on such anharmonic $(0,0,n \rightarrow 0,0,n-1)$ transitions^{6,13} in CO_2 discharges have been unsuccessful. As the wavelength of such transitions extends from $4.3\text{ }\mu\text{m}$ to at least $4.7\text{ }\mu\text{m}$ (see Section 2, Table 1), such laser action is attractive for several avionics applications. In the present program, a broader investigation of the laser potential of this system was undertaken. A principal program task was to verify and extend the

results of Ref. 13. In Ref. 13, Dang, et al. only measured the ν_3 populations from (00^01) to (00^09) . The measurement technique used, tunable diode laser absorption, precluded measurement above (00^09) , as the diode could not be tuned to sufficiently long wavelengths corresponding to the absorption band for these higher components. In the present experiments, the primary diagnostic is infrared emission spectroscopy. Significant populations of levels above (00^09) can be detected. A second program task was investigation of the effect of discharge operating parameters (gas temperature, flow velocity, gas mixture, current) on the partial inversion in the ν_3 states. Finally, attempts were made to achieve laser oscillation under the most favorable pumping conditions. These efforts were unsuccessful.

Section II, following, reviews the previous experimental findings important for the present project, and presents gain calculations for the system. Section III gives the measurements of populations, and the results of both parametric studies of the discharge operation and laser oscillation attempts. A summary and conclusions are in Section IV.

Section II

CO₂ (ν_3) MODE POPULATION DISTRIBUTIONS AND CALCULATED SMALL SIGNAL GAIN

Dang, et.al.¹³ have performed detailed vibrational population distribution measurements of the CO₂ ν_3 mode (00n) states from n = 0 to n = 9, in a 10 cm long x 1 cm bore, wall-cooled discharge tube. The tube was operated at a relatively fast pump rate, 840 ml/min NTP, to minimize CO₂ dissociation. The CO₂ (00n) populations were measured by absorption of a tunable diode laser beam; this probe beam was directed down the axis of the discharge tube, and was restricted to a diameter of 2 mm in the center of the discharge tube bore by use of an iris. Further details are given in Ref. 13.

Figure 1 shows the CO₂ (00n) populations measured by Dang, et.al.¹³ with this technique. The discharge conditions are shown on the figure; this case represents the most highly pumped partial population inversion achieved. Measurements were made only up to level n = 9, since the diode laser could not be tuned to the wavelengths of transitions above (0,0,9) \rightarrow (0,0,10); it appears probable that the V-V pumped plateau extends to considerably higher quantum levels.

Shown on Fig. 1 is the analytical V-V pumped distribution function of Treanor, et.al.¹¹ (solid line); the agreement with the measured populations for $0 \leq n \leq 9$ is excellent. This analytical function is calculated for the measured translational temperature of $T_{\text{trans}} = 350^\circ\text{K}$ and for the measured vibrational "temperature" $T_{V_3}^*$ of 2850°K defined by the measured ratio of the (000) and (001) populations,

$$T_{V_3}^* = \frac{E(0,0,1) - E(0,0,0)}{k \ln [N(0,0,0) - N(0,0,1)]} .$$

For these conditions, the theory predicts the minimum of the V-V pumped analytical solution to occur at $V = 12$, as shown on the figure. Beyond this minimum, the analytic theory of Treanor, et.al.¹¹ predicts a total inversion, as shown by the solid-line curve; however, it has been well established that vibrational-to-translational (V-T) energy transfer processes generally inhibit such creation

of total inversions, and that the actual distribution function beyond the minimum at $V = 12$ can be approximated by the form $N_V \approx \text{CONSTANT} \times V^{-1}$.¹⁴ This form is shown for $V \geq 12$ as the dashed line in Fig. 1; it forms a reasonable prediction of the distribution that would be measured by an experimental diagnostic giving access to the states $V > 9$.

On the basis of this predicted distribution function for the higher anharmonic CO_2 ($00n$) states, it is possible to estimate the small signal gain that can be achieved on $(0,0,n) \rightarrow (0,0,n-1)$ transitions. Figure 2 shows such a calculation for the peak of a Doppler-broadened gain profile. The small-signal gain expression used is that of Patel;¹⁵ it is written out explicitly on the figure. The gains for the $(0,0,16) \rightarrow (0,0,15)$ band component are calculated for the distribution of Fig. 1 and for the CO_2 concentration of the Dang, et.al., experiment ($P_{\text{CO}_2} = 0.31$ torr). Gain is plotted against J' , the rotational quantum number of the upper level in the transition. The sources of the molecular constants and transition probabilities used in this estimate are also shown on the figure. Gains are plotted for 350°K, the temperature of the experiment, and for two lower temperatures, 250° and 150°K.* It can be seen that gain is very slight for the 350°K temperature of the experiment of Ref. 13, even on the $(0,0,16) \rightarrow (0,0,15)$ band; gain is smaller or non-existent for the lower-order transitions. This conclusion is in accordance with the results reported by Dang, et.al., who were unable to measure any gain on the $(00^9) \rightarrow (00^8)$ transition for these conditions.

While Fig. 2 indicates that gain is considerably higher at kinetic temperatures of 150°K and 250°K than for 350°K, it is important to realize that these results are all based on the distribution of Fig. 1, which was measured at 350°K. Theory and experiments in several V-V pumped molecular species¹⁶ indicates that a more strongly pumped population distribution is created for the same power input at the lower kinetic temperatures. Such distributions can be predicted with some confidence on the basis of the analyses

* The CO_2 vapor pressure at 150°K is > 1 mm Hg.

already cited.^{11,14} Such distributions are shown in Fig. 3. As indicated on the figure, the distributions are calculated for $T_{V_3}^* = 2850^\circ\text{K}$, the value measured in Ref. 13, but for $T_{\text{TRANS}} = 150^\circ\text{K}$ and 250°K , as well as 350°K . The 350°K distribution is the same as that inferred previously (Fig. 1); the more highly populated inversions predicted by theory for the two lower temperatures are apparent.

Small signal gains calculated from the distributions of Fig. 3 are displayed in Fig. 4 (250°K) and Fig. 5 (150°K). For the 250°K case, gain approach $1\% \text{ cm}^{-1}$ for the higher band components; for 150°K , gain on all bands above $(00^05) \rightarrow (00^04)$ exceeds $1\% \text{ cm}^{-1}$, approaching $10\% \text{ cm}^{-1}$ for the higher band components. It is also noteworthy that partial inversion occurs on the lower band components as the temperature is lowered; for the 150°K case, high gain is predicted from $4.5 \mu\text{m}$ to above $5.0 \mu\text{m}$ (cf. Table 1).

Finally, it should be noted that the recent observation of extreme V-V pumping of the $\text{CO}_2 \nu_3$ mode of Ref. 13 is not the only observation of such pumping in a triatomic molecule. Several years ago, Picard-Bersellini and Rossetti measured quite analogous pumping of the $\text{N}_2\text{O } \nu_3$ mode asymmetric stretch populations in $\text{N}_2/\text{N}_2\text{O}$ mixtures in a mixing discharge tube.¹⁷ This independent observation in a different triatomic species strongly supports the inferences drawn in Ref. 13.

Table 1
CO₂ ν_3 BAND WAVELENGTHS

V_3	$E_{0,0^0,V_3}$ (cm ⁻¹)	$\tilde{\nu}_{0,0^0,V_3 \leftrightarrow 0,0^0,V_3-1}$ (cm ⁻¹)	$\lambda_{0,0^0,V_3 \leftrightarrow 0,0^0,V_3-1}$ (μ m)
0	0	--	--
4	9,248	2275.	4.396
7	15,922.	2200.	4.545
10	22,370.	2125.	4.706
13	28594.	2050.	4.878
16	34592.	1975.	5.063
20	42240.	1875.	5.333

Section III

EXPERIMENTS

Experiments were conducted in a flowing gas discharge tube, with 150 cm of active length. In the course of the program two different tube diameters were used, 2 cm and 1 cm I.D. Premixed gases are fed into the tube through a central injection port, and are pumped through exhaust ports at each end. There is a central grounded electrode, and a positive electrode at each end. Accordingly, two discharge loops of 75 cm length are struck in the tube. The system is resistively ballasted in standard fashion, and powered by a Universal Voltronics 70 kV/110 ma regulated D.C. supply equipped with a saturable core reactive current limiter. The gases are pumped by a 500 liter/min mechanical pump. CaF_2 windows at each tube end allow spontaneously emitted endlight to be focussed into a scanning monochromator. The tube is equipped with a trough for liquid-nitrogen or dry ice/methanol wall-cooling baths along the entire active discharge length.

All spectra were taken with a 1/2 meter monochromator, equipped with a 300 line/m.m., 4 μ m blaze grating, and an InSb detector. Radiative signal was chopped at 800 Hz and amplified by a PAR 124 phaselock amplifier in standard fashion.

1 LARGE BORE TUBE

Figures 6-9 show typical endlight infrared emission spectra obtained from operation of the 2 cm I.D. tube. The molecular band spectra shown in these figures are the ν_3 , $(0,0^\circ,n) \rightarrow (0,0^\circ,n-1)$ band of CO_2 and the $\Delta V = 1$ fundamental band of CO. The CO is created by CO_2 dissociation in the discharge.

The experimental discharge conditions for each of Figs. 6-9 are given in Table 2.

Table 2
OPERATING PARAMETERS, 2 cm DIAMETER TUBE MEASUREMENTS

FIG.	FLOW VELOCITY m/sec	P _{CO₂}	P _{N₂} TORR	P _{He}	CURRENT mA	COOLING [*]
6	0.18	0.7	4.2	9.6	25	dry ice
7	10.1	0.15	1.5	17.0	22.5	room temperature
8	57.7	0.1	0.5	15.0	30.0	dry ice
9	46.4	0.3 ^{**}	0.6	14.9	22.5	liquid nitrogen

^{*} This column indicates the type of wall cooling bath. In Figures 7-9, gases were precooled additionally by passing through a dry ice methanol trap before injection into the discharge tube.

^{**} In this run, some CO₂ was being condensed on the discharge tube walls.

Figure 6 shows the IR spectrum for a relatively slow flow. The structure from 4.35 μ m to 4.45 μ m is the CO₂ ν_3 band. The structure beyond 4.45 μ m is almost entirely the CO fundamental band. It is interesting to note that almost all of the (001) and (002) emission is absorbed by atmospheric CO₂ in the optical path. The strong CO emission is evidence of almost complete CO₂ dissociation. The CO₂ ν_3 Einstein "A" coefficients exceed those of the CO fundamental by almost an order of magnitude.

Figures 7-9 show the IR spectrum for much faster gas flows. The almost total inhibition of CO formation, in contrast to Fig. 6, is evident. Figures 7-9 show the effect of decreasing translational temperature; in Fig. 7, the tube walls are at room temperature, in Fig. 8, they are at 193°K, and in Fig. 9, at 77°K.

Two features in the spectra are observed as the wall temperature is lowered. One is that the CO₂ ν_3 band components extend to longer wavelengths with decreasing temperature. In the case of Fig. 7, the room temperature case, there is little emission beyond 4.50 μ m, and the intensity drops perceptibly beyond 4.4 μ m. In the case of Fig. 9, the coldest run, emission extends to

almost $4.7\mu\text{m}$, and the intensity beyond $4.5\mu\text{m}$ is generally much greater with respect to the shorter wavelength emission, $\lambda < 4.50\mu\text{m}$.

A second feature created by the decreasing temperature is that the structure of the various band components becomes more evident. Particularly in Fig. 9, the alternating intensity rise and fall caused by the overlapping of the P and R branches of the successive $(0,0^0,v) \rightarrow (0,0^0,v-1)$ band components is apparent. This effect is obscured at the higher temperatures, where more rotational states are populated. These additional rotational lines tend to fill in the emission spectra, obscuring the band structure.

2 COMPARISON WITH COMPUTED SYNTHETIC SPECTRA

The Calspan synthetic spectrum computer code¹⁸ was used to generate synthetic spectra for the purposes of comparison with the experimental spectra of Figs. 7-9. Figures 10-12 show these spectra; they were generated for the three V-V pumped distributions theoretically calculated for 150°K , 250°K , and 350°K translational temperature, as plotted in Fig. 3.

Comparisons of Figs. 10, 11, and 12 shows the very marked increase in the predicted emission from longer wavelengths with decreasing translational-rotational temperature. The experimental spectrum of Fig. 9, the most highly pumped experimental case, has been compared with these theoretical predictions to estimate the magnitude of the partial population inversion achieved. Convenient reference points on the spectra, for the purposes of this comparison, are the emission peaks near 4.4 and $4.6\mu\text{m}$; these represent signal from $V_3 \approx 4$ and $V_3 \approx 8$, respectively. Table 3 shows the ratio of these emission peaks from the optimum experimental spectrum (Fig. 9), and from the three predicted spectra (Figs. 10-12).

Table 3
Emission Intensity Ratios

Case:	$I_{4.6}/I_{4.4}$
Experimental (Fig. 9)	0.42
Theoretical (Fig. 10)	0.85
Theoretical (Fig. 11)	0.44
Theoretical (Fig. 12)	0.19

It can be seen that the experimental distribution exhibits an emission intensity ratio quite close to that predicted theoretically for a vibrational population distribution with a translational temperature of 250°K (see Fig. 3). This is consistent with the temperature deduced from less direct experimental evidence. Experimental emission spectra such as that of Fig. 9 can be produced when the inlet gases to the discharge tube are precooled by a 193°K heat exchanger, and with the discharge tube walls also cooled to 193°K; cooling the tube walls to 77°K does not significantly increase the long-wavelength emission. Accordingly, it is reasonable to infer a 250°K centerline temperature in the tube, in agreement with the IR emission spectrum data.

Summarizing the results of these studies:

1. At the flow velocities used in the experiment of Dang, et al.¹³ (< 1 m/sec), a large fraction of the CO_2 is dissociated in the 75 cm length of each discharge section of the present experimental device. To ensure that most CO_2 does not dissociate, much higher flow velocities (> 10 m/sec) must be used. This finding is in accord with the detailed measurements of CO formation in CO_2 electric discharge lasers performed by Wiegand, et al.¹⁹
2. Cooling the gas discharge tube with wall baths, in addition to precooled the gases in a cold trap before they are admitted into the tube, results in marked enhancement of the V-V pumping of the CO_2 ν_3 mode vibrational states. This finding is in agreement with the theoretically predicted CO_2 ν_3 mode population distributions given in the calculations of Section 2.
3. Populations of the CO_2 ν_3 states up to $(0,0^0,10)$ have been measured.

Infrared emission spectra have also been obtained using 1 cm I.D. tube; this smaller diameter was tested to ascertain if lower center-line temperatures could be achieved with wall-cooling than in the 2 cm I.D. system. Figures 13-16 show the endlight emission spectra obtained with this tube; the discharge operating parameters for these cases are given in Table 4.

Table 4
Operating Parameters

FIG.	FLOW/VELOCITY m/sec	P _{CO₂}	P _{N₂} TORR	P _{He}	CURRENT mA	COOLING
13	147	0.37	1.2	21.4	30	Dry ice
14	129	0.39	0.76	15.7	22.5	Liquid nitrogen
15	147	0.37	1.2	21.4	30	Dry ice
16	169	0.33	1.1	18.6	10	Dry ice

Figures 13 and 14 show the spectra for, respectively, dry ice and liquid nitrogen wall-cooling. No substantial pumping improvement over the 2 cm I.D. tube experiments is noted.

As noted earlier, the emission spectra all show substantial absorption of the CO₂ (001 → 000) and (002 → 001) band components, caused by residual CO₂ in the optical instrumentation train. Since this effect did not impair the usefulness of the IR emission monochromator setup as a diagnostic for ν_3 mode V-V pumping, complete shrouding and purging of the apparatus was only used in a few runs. Such spectra, obtained with shrouded optics and with dry nitrogen gas purges passing through the shrouds and the monochromator, are given in Figs. 15 and 16. It can be seen that substantial emission due to (002 → 001) and (001 → 000) transitions is recovered, in contrast to the spectra obtained with the unpurged instrumentation. Both Figs. 15 and 16 are for dry ice in alcohol wall cooling baths. It will be noted from Table 4, however, that Fig. 15 is for a current of 30 mA (current density = 38 mA/cm²), while Fig. 16 is for a current of 10 mA (current

density = 13 mA/cm^2). The high current density run (Fig. 15) clearly shows much higher rotational temperature than the low current density case (Fig. 16). Comparison of Fig. 15 with synthetic spectra indicate translational/rotational temperatures $> 400^\circ\text{K}$; in the case of Fig. 16, translational/rotational temperatures $\sim 250^\circ\text{K}$ are achieved; Fig. 16 is quite close to the 250°K distribution which gives the synthetic spectrum of Fig. 8. We note that the lower current densities required to prevent translational heating in the 1 cm tube are difficult to achieve at these high flow velocities required to inhibit dissociation. Currents lower than 10 mA gave unstable discharge operation, with a tendency for one or both discharge arms to extinguish. Accordingly, as noted above, no substantial improvement over the 2 cm bore results have been realized. A configuration to eliminate this difficulty to small bore operation is suggested in Section 4.

4 GAIN ESTIMATES AND LASER OSCILLATION EXPERIMENTS

The emission spectra for the "best-pumped" cases of Figs. 9 and 16 correspond closely to the synthetic spectrum of Fig. 11 for the 250°K theoretical distribution of Fig. 3, for states below $(0,0^0,10)$. Gains inferred for this distribution are low among these lower states. As shown on Fig. 4, gains on the $V_3 = 9 \rightarrow 8$ transition range from $3 \times 10^{-3} \text{ cm}^{-1}$ on P_3 , to $1 \times 10^{-3} \text{ cm}^{-1}$ on P_{27} , per torr of CO_2 . Accordingly, for the CO_2 pressures run here, maximum anticipated gain is rather low, of the order of 10% per pass in the 150 cm tube.

Tests for laser oscillation were performed in both the 1 cm and 2 cm I.D. tubes. An optical cavity was formed by dielectric-coated mirrors, a max-reflectance mirror with 99.9% reflectance in the $4\text{--}5 \mu\text{m}$ range, and a partially-transmitting mirror with $>96\%$ reflectance from 4.5 to $4.8 \mu\text{m}$. No CO_2 laser oscillation was obtained for the conditions giving the optimum pumped distribution of Figs. 9 and 14. Precise alignment was checked using CO in the laser cavity; despite the fact that the optics were unoptimized for CO laser action, ~ 3 watts c.w. were easily obtained on CO lines.

For both tube diameters, discharge operating parameters (current density, $\text{CO}_2/\text{N}_2/\text{He}$ partial pressures, flow velocity) were varied over large ranges

around the values giving the pumped emissions of Figs. 9 and 14. We were still unable to force laser oscillation.

Section IV

SUMMARY AND CONCLUSIONS

Measurements have been made of the vibrational population distribution of the CO_2 asymmetric stretch mode, in a flowing glow discharge, using quantitative infrared emission spectroscopy of the $\text{CO}_2 \nu_3 (0,0,V) \rightarrow (0,0,V-1)$ bands. These $\text{CO}_2 \nu_3$ states from (001) to (009) are in a V-V pumped distribution at the lower discharge current densities, in agreement with the earlier results of Dang, et al.

It was found that in discharge tubes of length sufficient to yield usable total gain for optimum V-V pumping, a large fraction of the CO_2 dissociated for the flow velocities of Ref. 13. High flow velocities were required to inhibit dissociation.

IR monochromator scans were made in the wavelength region from $4.7 \mu\text{m}$ to $5.1 \mu\text{m}$. The $(0,0,11) \rightarrow (0,0,10)$ to $(0,0,16) \rightarrow (0,0,15)$ $\text{CO}_2 \nu_3$ band components lie in this region. No emission from these band components could be detected. If these higher $\text{CO}_2 \nu_3$ states were populated to the extent predicted by the V-V pumped models given in Fig. 3, they would have been readily detectable with the instrumentation used. It is concluded that the $\text{CO}_2 \nu_3$ does not continue to V-V pump strongly above (0,0,10).

With the wall-cooling and pre-cooling methods used for the discharge gases, the minimum center line translational temperatures achieved were $\sim 250^\circ\text{K}$, for usable discharge current densities ($> 15 \text{ mA/cm}^2$). At lower current densities, the discharge became unstable. Lower center line translational temperatures (and lower current densities) could be achieved in the present apparatus at slower flow velocities; however, this results in a prohibitively large fraction of CO_2 dissociation. Therefore, the present wall-cooled, 75 cm per arm discharge could not practically be operated below $\sim 250^\circ\text{K}$.

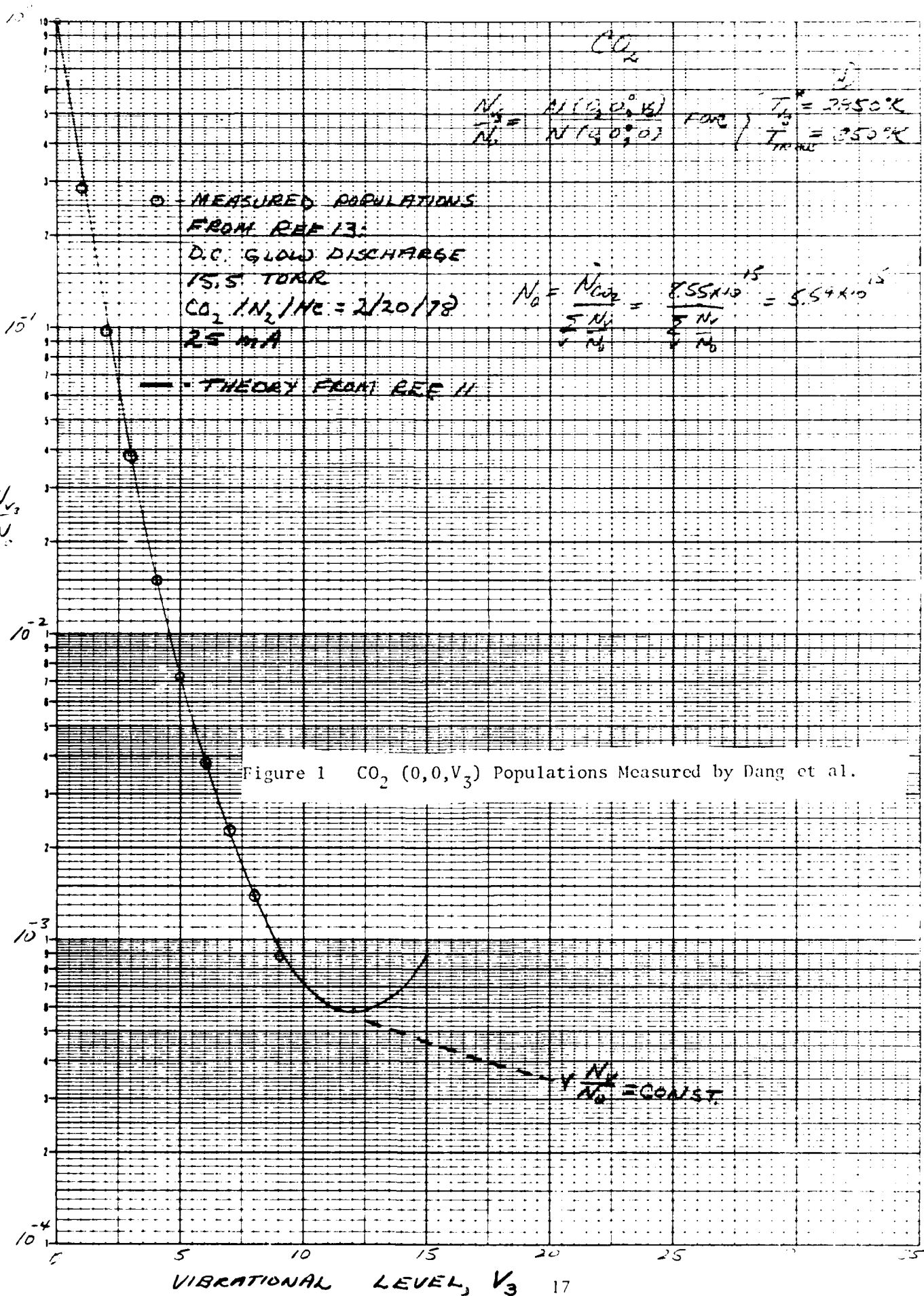
Among states $\text{CO}_2 (0,0,10)$ to $\text{CO}_2 (0,0,1)$ at a 250°K translational temperature, maximum gains realized were estimated to be of the order of .05% per cm (on the $(009) \rightarrow (008) P_{31}$ transition). Despite the low estimated gains, laser oscillation tests were conducted. It was not possible to force laser oscillation, although discharge operating parameters were systematically varied in an effort to increase gain.

It is concluded that $\text{CO}_2 \nu_3$ mode lasing is not achievable in a wall-cooled glow discharge apparatus of the type used in the present study. This is because levels above (0,0,10) do not V-V pump, and lasing among levels (0,0,9) and below requires lower translational/rotational temperatures than can be achieved at the flow rates required to inhibit CO_2 dissociation.

$\text{CO}_2 \nu_3$ mode oscillation may well be achievable in alternate laser geometries. For example, a segmented discharge tube, consisting of several short (15 cm) discharge sections, each having separate gas injection and removal, would allow much lower flow velocities and consequent efficient wall cooling, resulting in lower gas translational/rotational temperatures. At the same time, CO_2 dissociation would be minimal in each section. A second approach would be to explore aerodynamic expansion methods of gas cooling. Both of these alternatives have the disadvantage of adding to the system complexity, in contrast to single discharge tube devices.

REFERENCES

1. Osgood, R., Appl. Phys. Lett. 28, 342 (1976).
2. Manuccia, T.J., Stregack, J., Harris, N., and Wexler, B., Appl. Phys. Lett. 29, 360 (1976).
3. Kasner, W.H., and Pleasance, L.D., Appl. Phys. Lett. 31, 82 (1977).
4. Buchwald, M.I., James, C.R., Fetterman, H.R., and Schlossberg, H.A., Appl. Phys. Lett. 29, 300 (1976).
5. Reid, J., and Siemsen, K., Appl. Phys. Lett. 29, 250 (1976).
6. Reid, J., and Siemsen, K., J. Appl. Phys. 48, 2712 (1977).
7. Feldman, B.J., Fisher, R.A., Pollock, C.R., Simons, S.W., and Tercovich, R.G., Opt. Lett. 2, 166 (1978).
8. Znotins, T.A., Reid, J., Garside, B.K., and Ballik, E.A., Optics Lett. 4, 253 (1979).
9. Bertel', I.M., Petukhov, V.O., Stepanov, B.I., Trushin, S.A., and Churakov, V.V., Sov. Phys. Dokl. 25, 1009 (1980).
10. Znotins, T.A., Reid, J., Garside, B.K., and Ballik, E.A., Appl. Phys. Lett. 39, 199 (1981).
11. Treanor, C.E., Rich, J.W., and Rehm, R.G., J. Chem. Phys. 48, 1798 (1968).
12. Rich, J.W., J. Appl. Phys. 42, 2719 (1971).
13. Dang, C., Reid, J., and Garside, B.K., Appl. Phys. B. 27, 145 (1982).
14. Caledonia, G.E., and Center, R.A., J. Chem. Phys. 55, 552 (1971).
15. Patel, C.K.N., Phys. Rev. 136, A1192 (1964).
16. Bergman, R.C., Williams, M.J., and Rich, J.W. Chem. Phys. 66, 357 (1982).
17. Picard-Bersellini, A., and Rossetti, C., Chem. Phys. Lett. 36, 647 (1975).
18. Rich, J.W., Bergman, R.C., and Williams, M.J., "Measurement of Kinetic Rates for CO Laser Systems" Final Report, AFOSR Contract No. F49620-77-C-0020, November, 1979, pgs. 27-29.
19. Wiegand, W.J., Fowler, M.C., and Benda, J.A., Appl. Phys. Lett. 16, 237 (1970).



1. χ^2 (chi)
 2. χ^2 (chi)
 3. χ^2 (chi)

LOGARITHMIC • 2 CYCLES X 70 DIVISIONS
• ESSER CO.
MADE IN U.S.A.

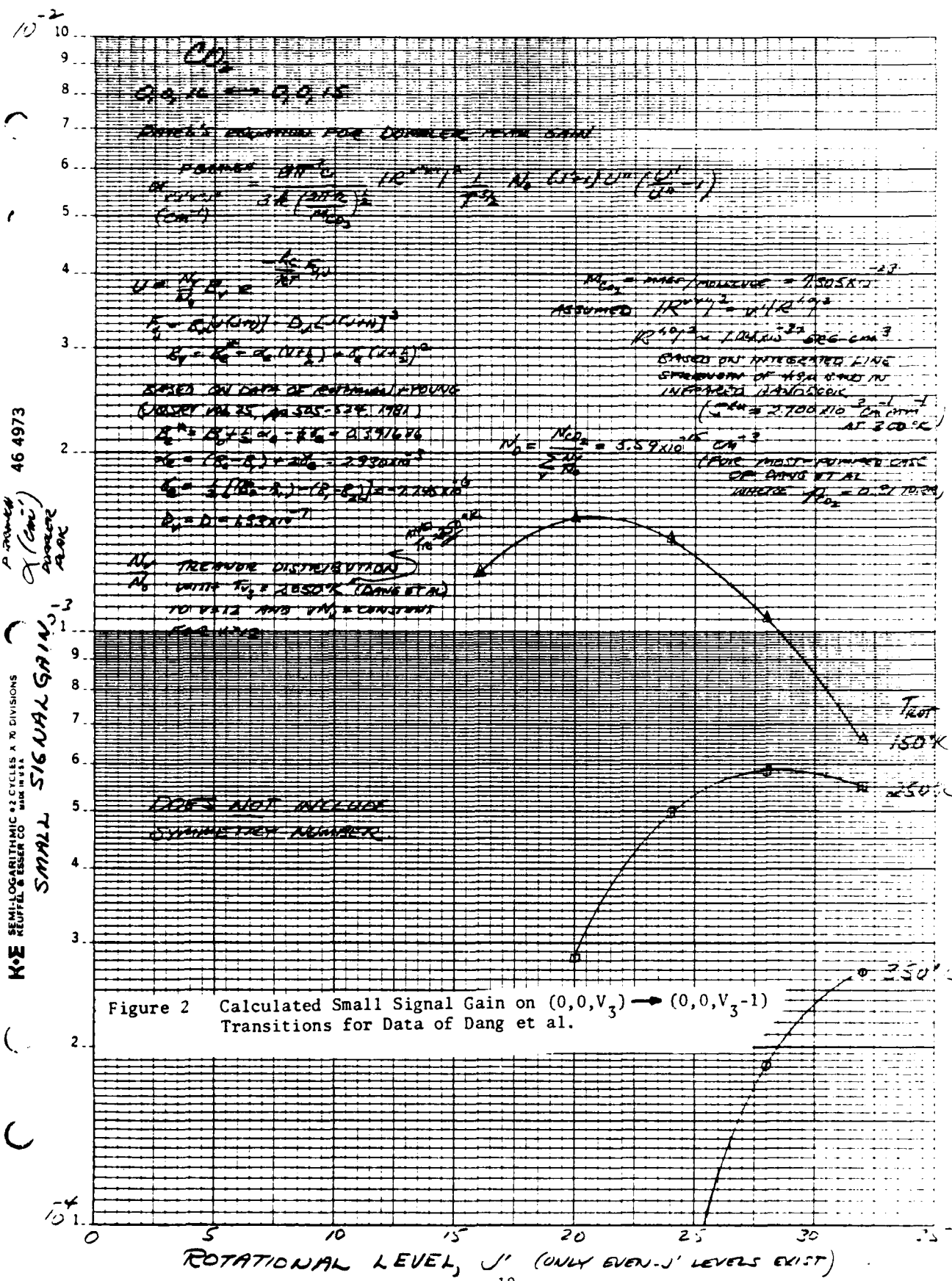
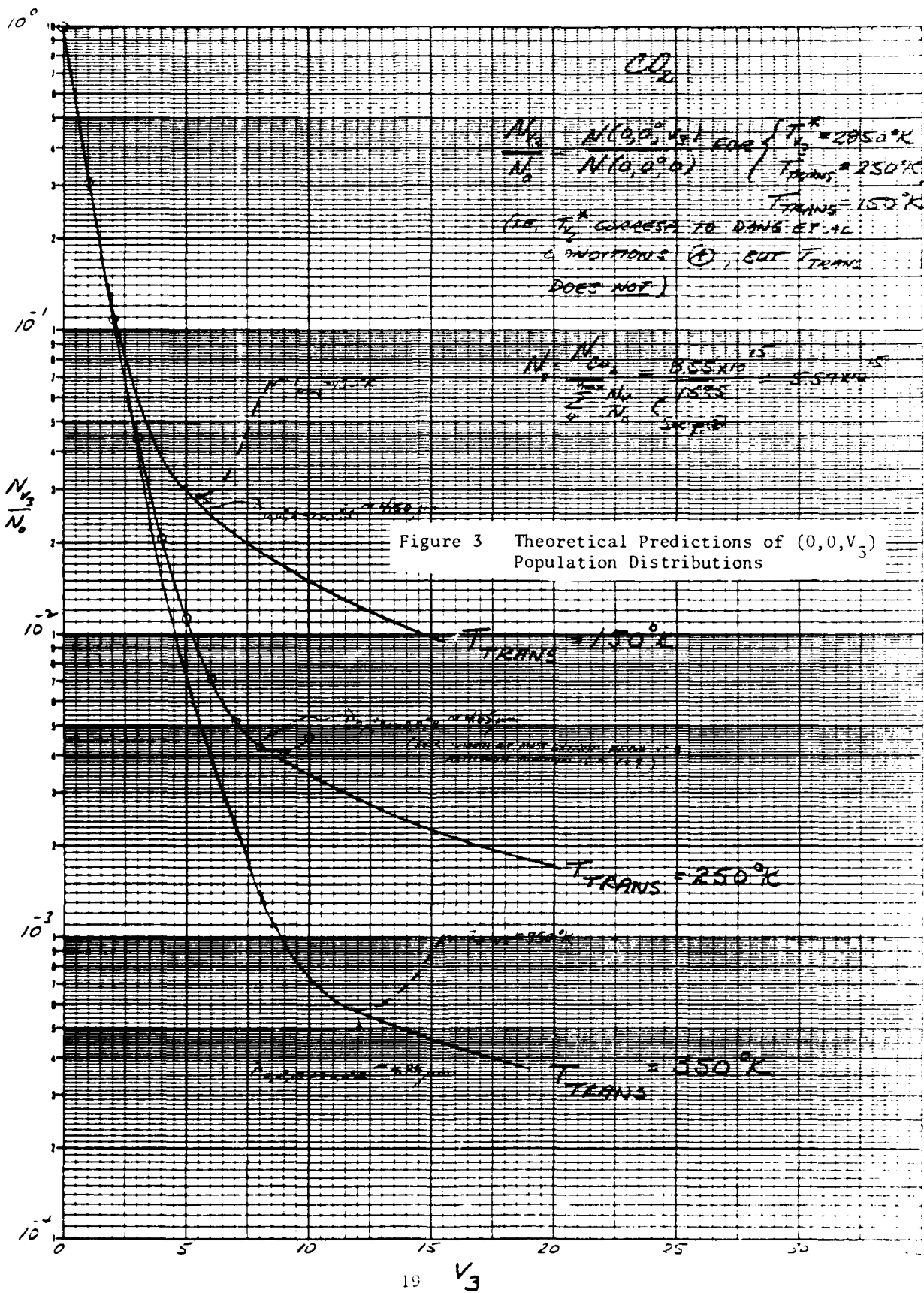
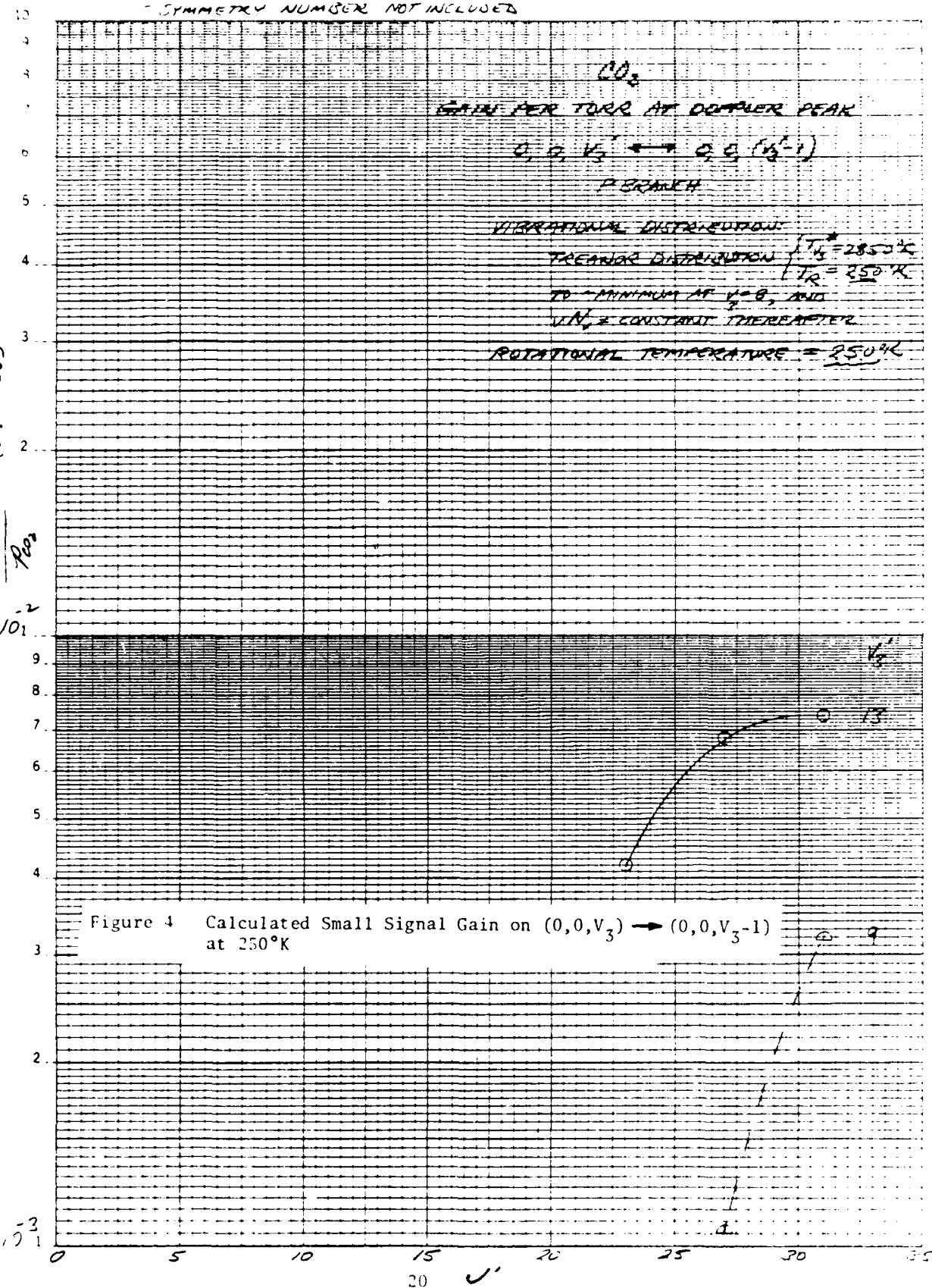


Figure 2 Calculated Small Signal Gain on $(0,0,V_3) \rightarrow (0,0,V_3-1)$ Transitions for Data of Dang et al.



- FOR $v_3 = \begin{cases} \text{EVEN} \\ 000 \end{cases}$, $v = \begin{cases} \text{EVEN} \\ 000 \end{cases}$
 - SYMMETRY NUMBER NOT INCLUDED



PAPER 464973
 COMPLEX AMPL (CM/1000)

K-E SEMI-LOGARITHMIC 1/2 CYCLES X 10 DIVISIONS
 REUFEL & ESSER CO. MADE IN U.S.A.

- FOR $V_3 = \begin{Bmatrix} \text{EVEN} \\ 000 \end{Bmatrix}$, $J = \begin{Bmatrix} \text{EVEN} \\ 000 \end{Bmatrix}$
- SYMMETRY NUMBER NOT INCLUDED

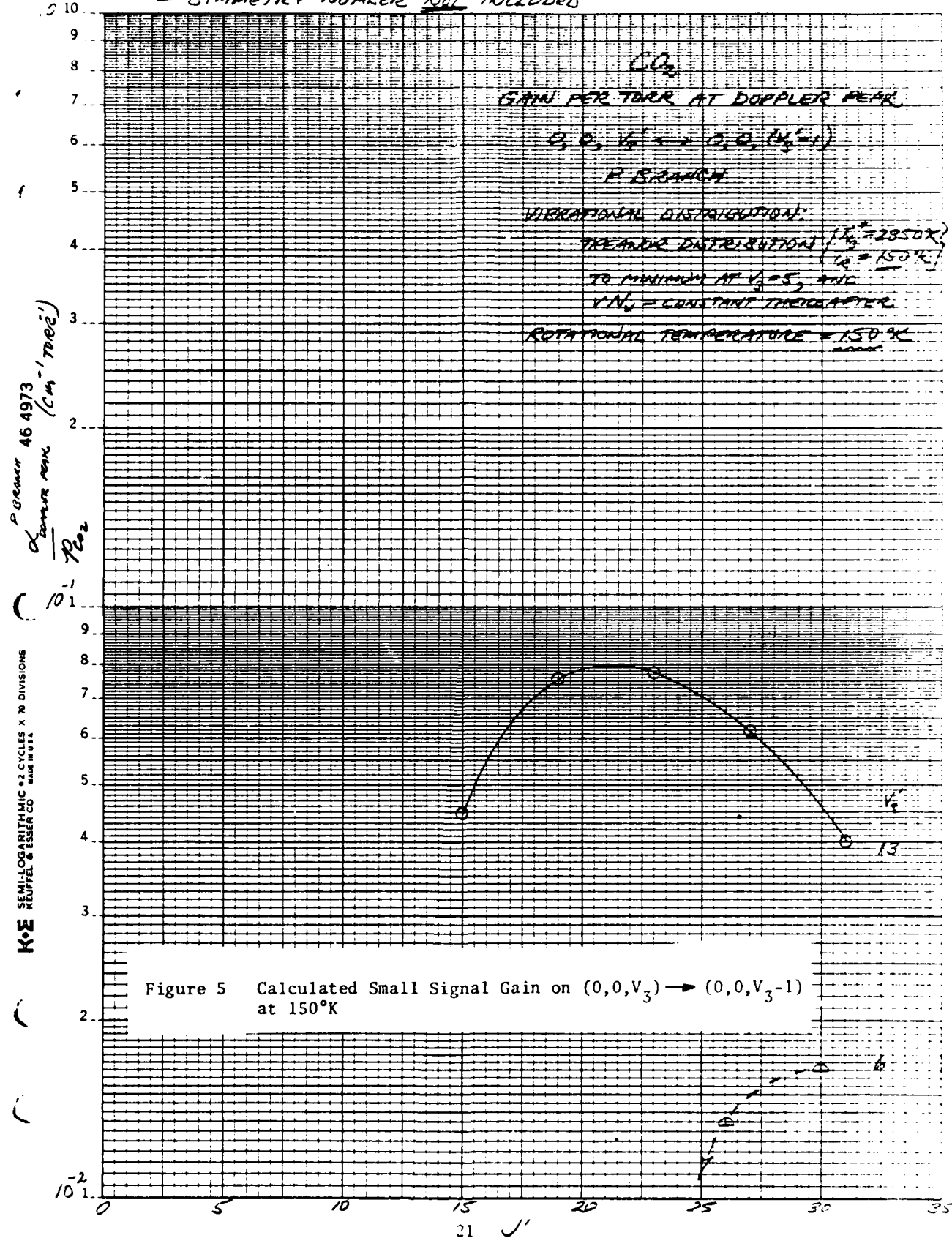


Figure 6 IR Emission Spectrum, 2 cm Tube, Slow Flow

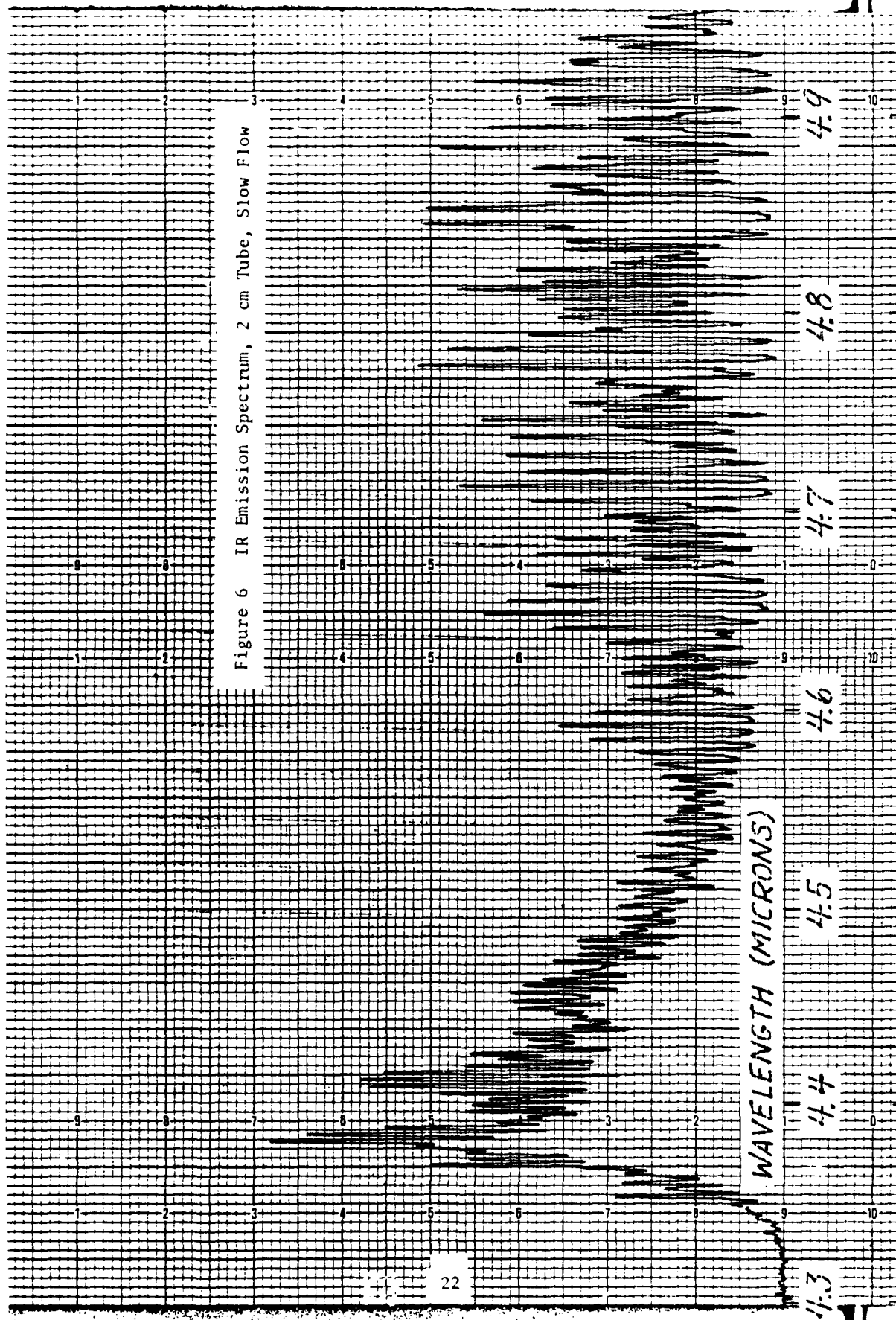


Figure 7 IR Emission Spectrum, 2 cm Tube, Room Temperature

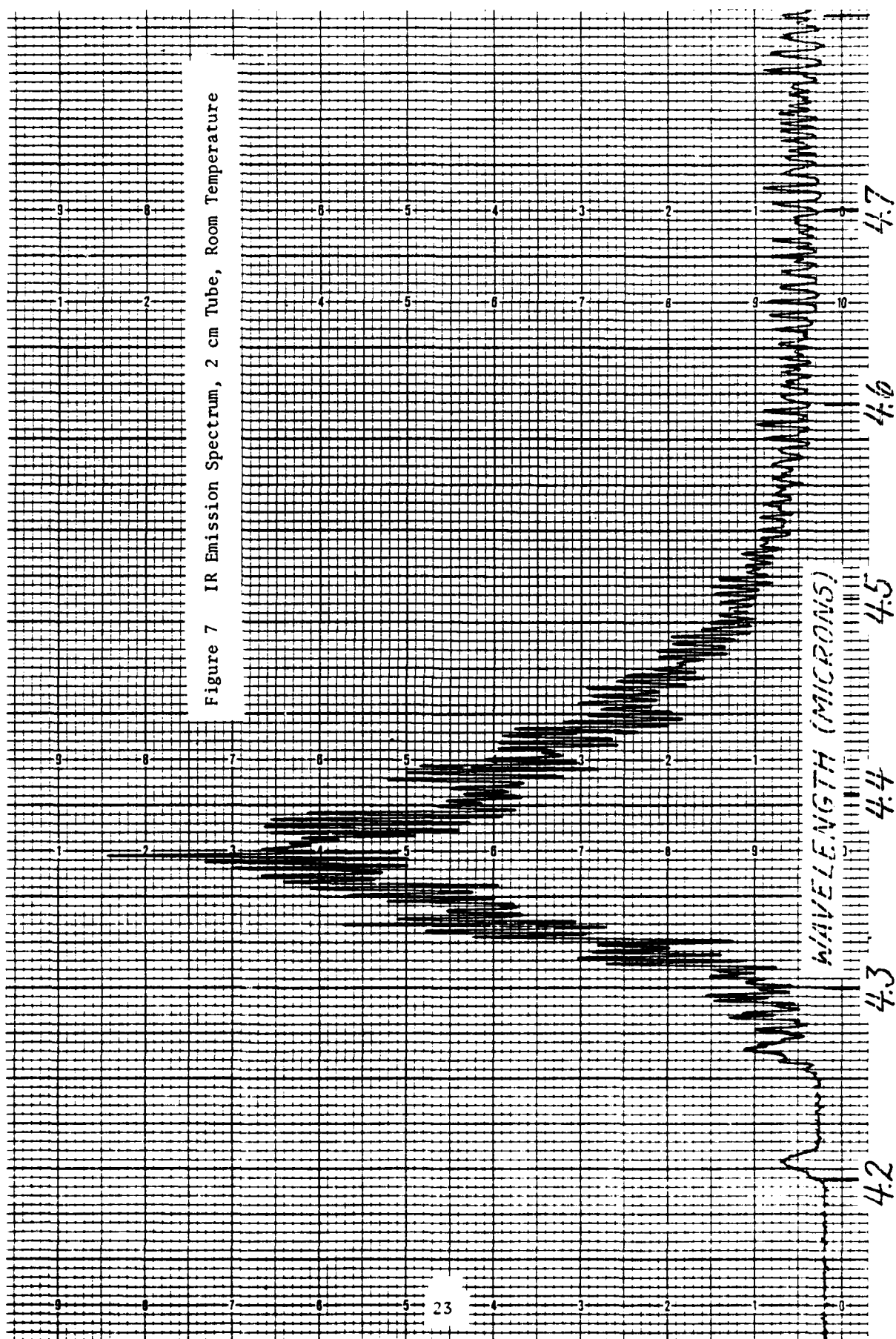


Figure 8 IR Emission Spectrum, 2 cm Tube, Dry Ice Cooling

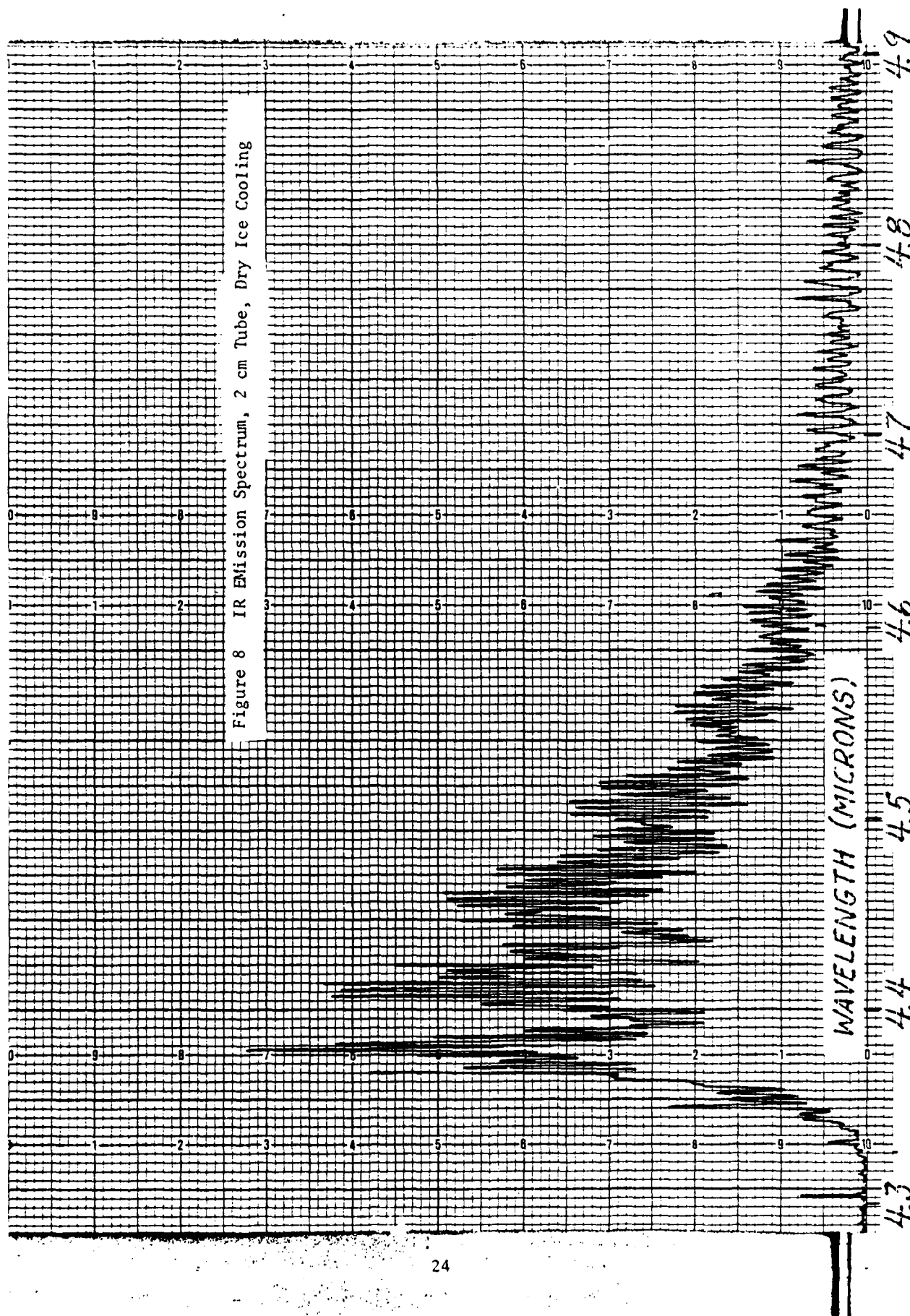


Figure 9 IR Emission Spectrum, 2 cm Tube, Liquid Nitrogen Cooling

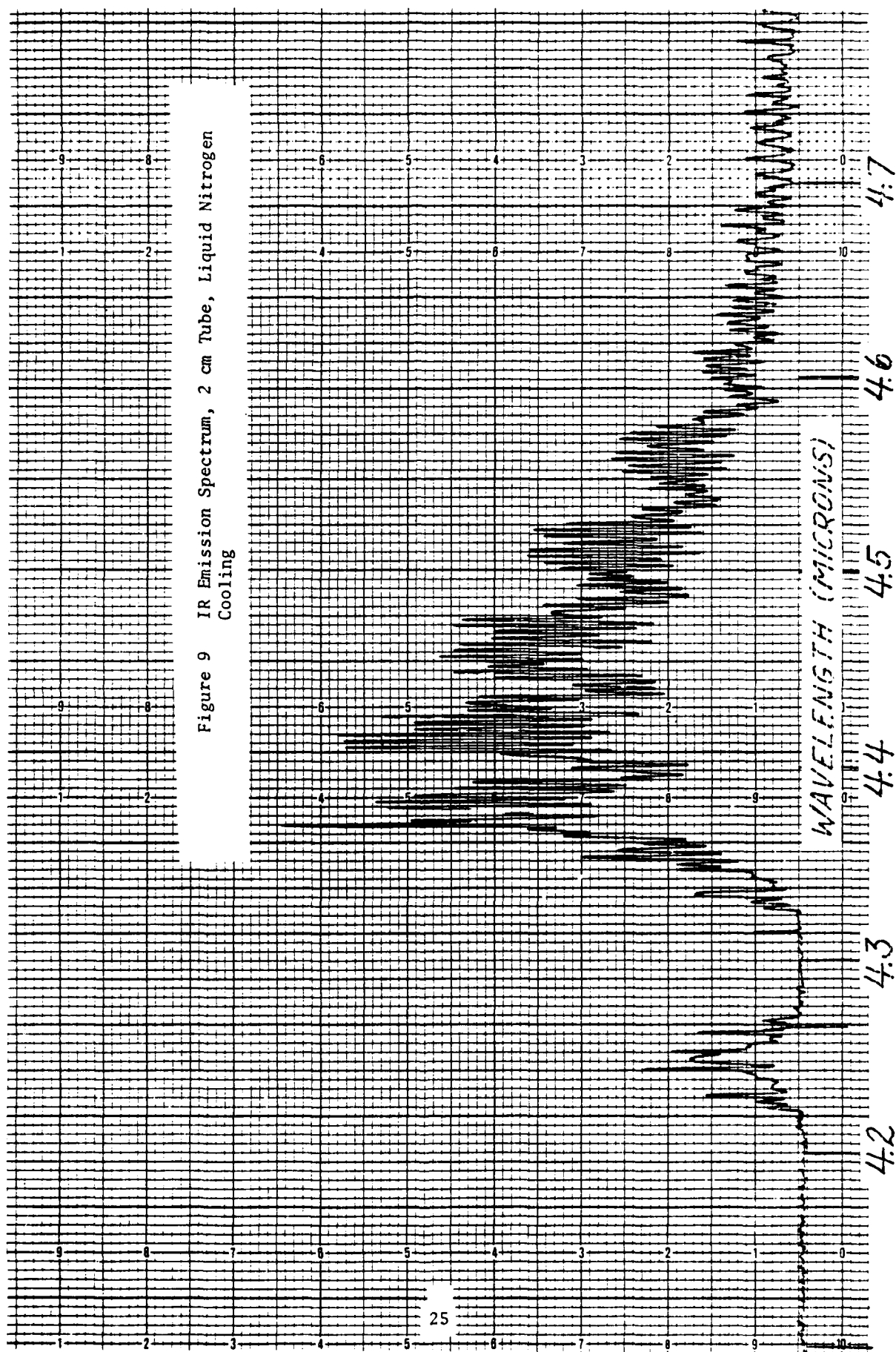


Figure 10 Synthetic CO₂ (ν_3) IR Spectrum for 150°K

$$T_{\text{TRANS}} = T_{\text{ROT}} = 150^\circ\text{K}$$

4.15 4.20 4.25 4.30 4.35 4.40 4.45 4.50 4.55 4.60
WAVELENGTH (MICRONS)

Figure 11 Synthetic CO₂ (ν_3) IR Spectrum for 250°K

$T_{trans} = T_{rot} = 250^\circ K$

4.15 4.20 4.25 4.30 4.35 4.40 4.45 4.50 4.55 4.60
WAVELENGTH (MICRONS)

Figure 12 Synthetic CO₂ (ν_3) IR Spectrum for 350°K

$T_{\text{TRANS}} = T_{\text{REF}} = 350^\circ\text{K}$

4.15 4.20 4.25 4.30 4.35 4.40 4.45 4.50 4.55 4.60
WAVELENGTH (MICRONS)

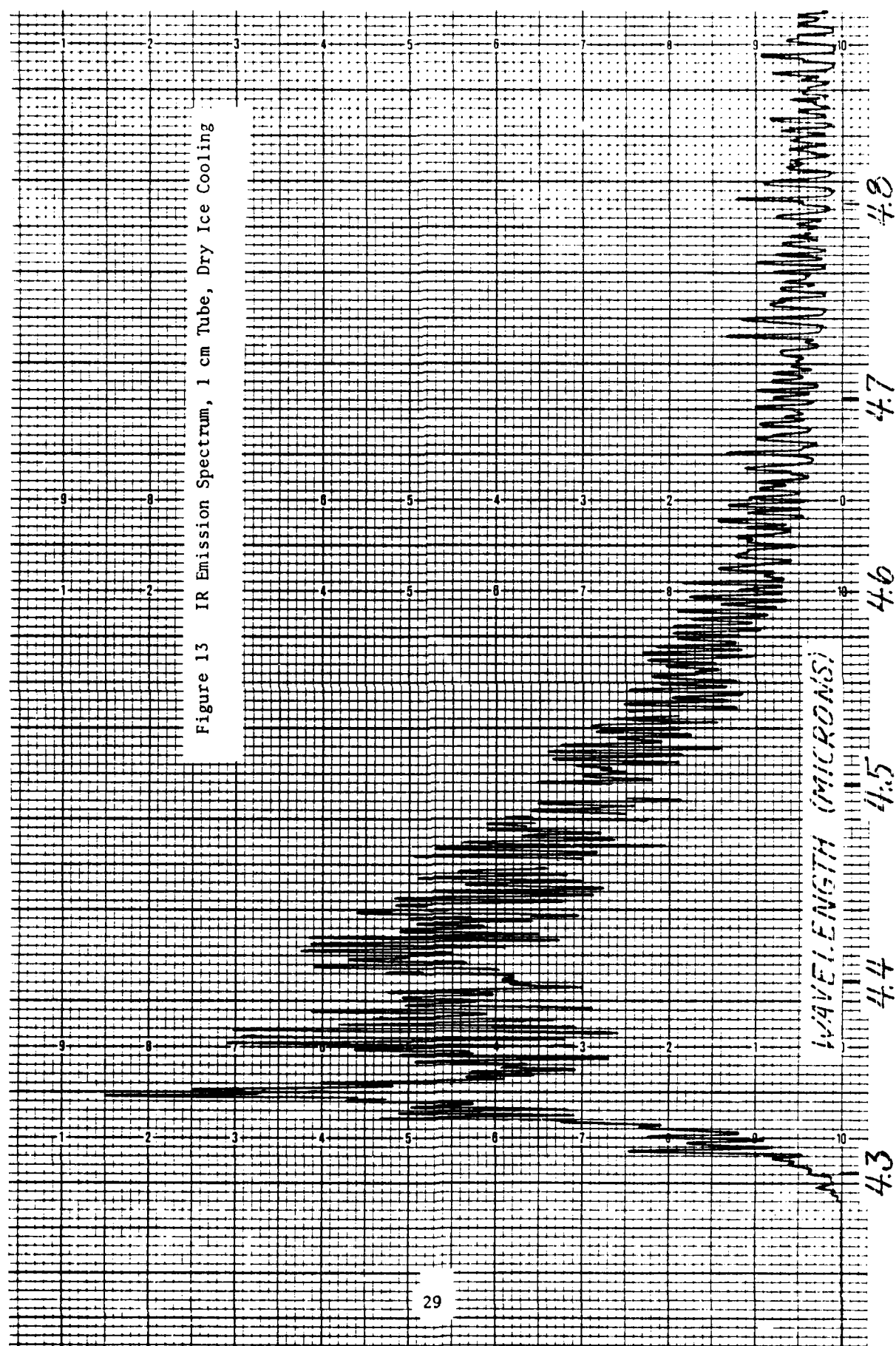
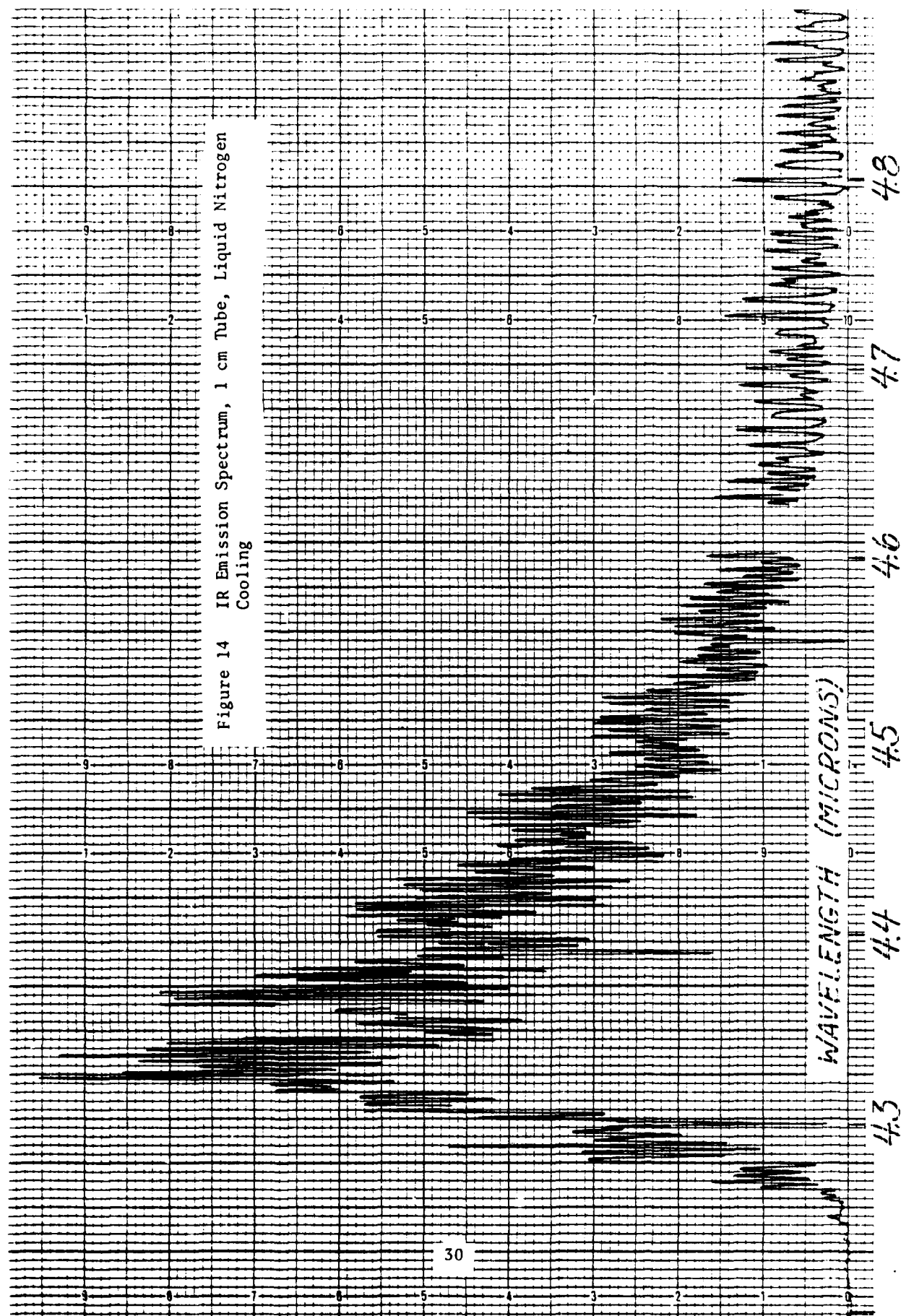


Figure 14 IR Emission Spectrum, 1 cm Tube, Liquid Nitrogen Cooling



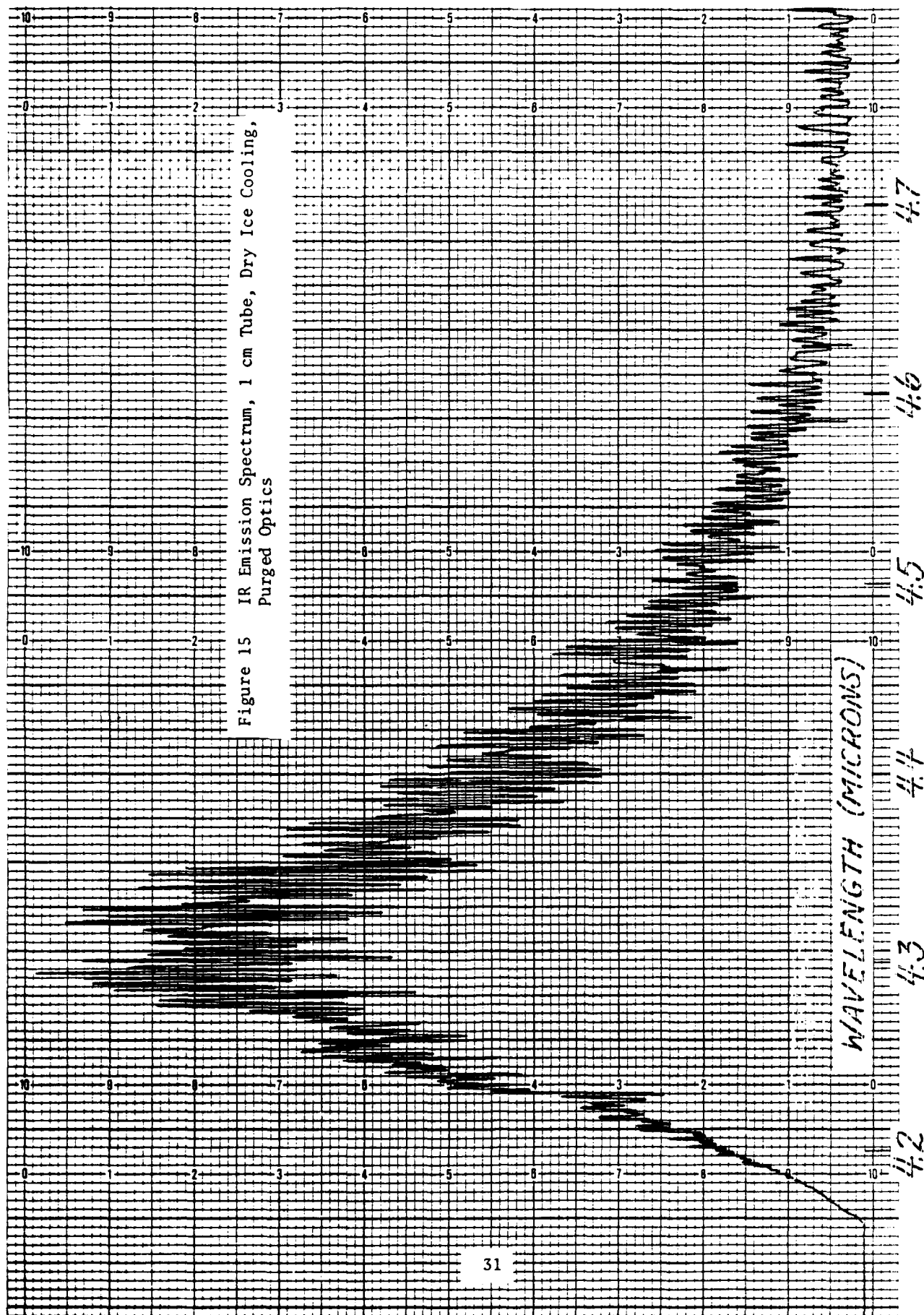
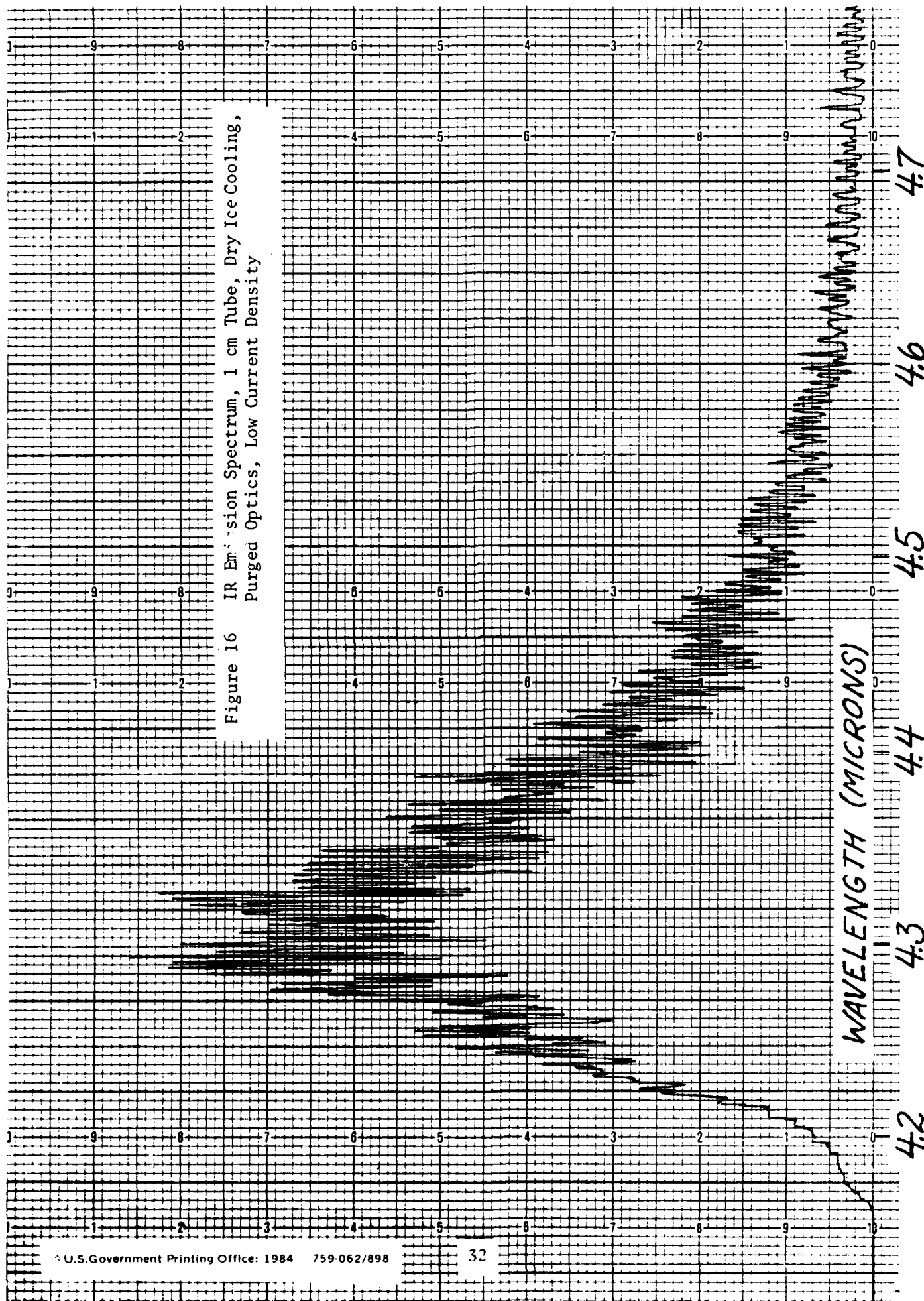


Figure 16 IR Emission Spectrum, 1 cm Tube, Dry Ice Cooling,
Purged Optics, Low Current Density



END

FILMED

8

74